# Environmental Effect on Fatigue Behavior of Epoxy Coating Used for Water Tanks

**Haider Hadi**
*Chemical Engineering Department, College of Engineering, Basrah University, Basrah, Iraq.*

The fatigue limit and lifetime of epoxy-based coatings may be affected by various factors, especially the environmental effects. This paper evaluates the impact of air, potable water media, and pollution gases ($CO_2$, $H_2S$, and $SO_2$) on the fatigue performance of two types of epoxy-based coatings (polyamine and polyamide epoxy-based coatings) used as lining for potable water storage tanks. The fatigue test apparatus is assembled in the laboratory and utilized for testing. Different factors are discussed, including absorption, adsorption, and the reaction of environmental gasses with polyamine and polyamide coating surfaces. The influence of porosity on the epoxy-based coatings is experimentally determined, and its effects on fatigue limit and fatigue life are discussed in detail. As a result, the coatings were applied to improve the fatigue resistance of stainless steel. The fatigue limits of both types of coatings tested in potable water are lower than the value obtained when tested in air or gas environments. The fatigue limit of polyamine coating is greater than the polyamide coating. The microscopic inspection indicated a different mechanism for initiating fatigue crack, and the test environments are affected by the nature of the fracture surface.

Keywords: epoxy coating; fatigue limit; diffusion; porosity; AISI 316 steel

## Introduction

Two types of large tanks (elevated and ground-based resting tanks) are usually used and spread throughout Iraq cities to store the drinking water. Corrosion, fatigue, and vibration are the essential issues of these tanks (Edward *et al.*, 2018). These tanks are built by welding plates manufactured from different kinds of stainless steel like AISI 316, AISI 316L, and ASTM 304 (Ignatius *et al.*, 2017). Most types of welding processes in stainless steel introduce a readily hydrogen-embrittled phase. The Hydrogen embrittlement of stainless steel affects fatigue behavior and fails lower loads and shorter times (Bruck *et al.*, 2018, Kumar *et al.*, 2013). The Hydrogen embrittlement of welding stainless steels can be prevented by minimizing contact b*et*ween the stainless steels and hydrogen, particularly during the welding process.

The epoxy coating application is implemented as an excellent technique of protecting these tanks from gaseous and water impacts. A drinking water exposes the tanks to a compl*et*e continuous full and empty cycle. This display of stresses and strains in coatings reaches greater values when filled and lower when tanks are empty, leading to fatigue and cracked coatings (Avery *et al.*, 1999). On the other side, the gaseous environment, mainly $CO_2$, $H_2S$, and $SO_2$ gases, will affect the stainless steel's resistance to fatigue and its applied epoxy coatings. Gas adsorptions on the material surface and metallurgical compositions are regarded as the main factors that affect the fatigue resistance of the material in gas media (Shan *et al.*, 2013). The rotating bending fatigue test is mostly used to evaluate steel's fatigue behavior and its applied coatings. The fatigue test results are drawn as a curve between cyclic stresses (S) and the number of cycles (N). The S-N curve allows the determination of the lifetime and fatigue limit properties of materials. The fatigue limit is characterized as the stress amplitude that can withstand material without fractures by applying infinite values of cycles. Several cycles of $10^7$ are chosen for metals and most polymer coatings to estimate the fatigue limit (Bensely *et al.*, 2009; Melia *et al.*, 2016, Nandiyanto *et al.*, 2019).

Multiple variables influence epoxy-based coating's fatigue properties, including porosity, the structure of the coating layer, absorption of water, and gaseous diffusion. Lukas *et al.*, (1982) researched the impacts of the environment gaseous in the growth, the spread of fatigue crack, and threshold value and showed that the effect of these gasses on the crack rate in austenitic steel is less than that for ferritic and martensitic steels. Sadananda *et al.*, (2000) provided a review of coating/substrate fatigue behavior. They showed that there are two types of fatigue damage depending on the range of cyclic loads applied.

Received on November 5, 2020; accepted on November 29, 2020; correspondence concerning this article should be addressed to Haider Hadi (E-mail address: raidhani73@yahoo.com ). ORCiD ID for Haider Hadi https://orcid.org/0000-0002-5560-1060

The first is the local fatigue damage, which is mostly linked to the surface, while the second is the general fatigue damage, which results from loads applied in a more extended range. Romero *et al.* (2012) estimated the various compounds in various epoxy paints that affect human health and safety. They indicated that the epoxy coatings used in covering drinking water tanks must be free of solvents that causing pollution of water and human health. Kurgan (2014) studied the mechanical and microstructure properties of AISI 316L stainless steel as a function of porosity density. Their results indicated that as porosity increases, the irregular pore formation tendencies also increased, affecting the mechanical properties. Foster (2015) studied the mechanisms processes of molecular failure of the epoxy-amine thermosets under the effects of mechanical fatigue. The experiment findings showed that the fatigue analysis generated radicals and a chain scission event in epoxy coating previous to failure. Kumar *et al.*, (2018) evaluated the distinct kinds of fatigue failures and variables affecting fatigue life of marine and naval structures. They mentioned numerous techniques for improving fatigue life. They showed that the fatigue life could be enhanced through distinct surface procedures, including coating, painting, grease oils, and mineral jellies. Wray *et al.*, (2018) studied the thermal cycling fatigue of welded steel ballast tank coatings at various temperature ranges. They discovered that the cracks formed at the weld line in the coatings and propagated it longitudinally. They also found that the cyclic numbers needed to generate cracks depended on the weld geometry and the coating thickness. Krauklis *et al.*, (2018) studied and described the fatigue resistance of amine-curing epoxy resin and the chemical structure changes due to the water impact. Their findings indicated the water absorption had reversible effects on the static and fatigue characteristics of amine cured epoxy resin. This paper evaluates the effects of gaseous air pollution, i.e., dry air, $CO_2$, $H_2S$, and $SO_2$ in Basrah province of south Iraq and potable water media in the fatigue limit, fatigue life, and strength of coated AISI 316 stainless steel. Two kinds of coatings based on epoxy used as a lining for potable water tanks are being studied. The fatigue test apparatus was collected in a laboratory and used for fatigue testing in different gases and water environments. In addition, the porosity of epoxy-based coatings is experimentally determined and studied its effects on fatigue behavior.

# 1 Materials and Methods

## 1.1 Epoxy based coating materials

The epoxy-based coatings consist of two separate, liquid-state sections (base and hardener) blended and left to cure on the tank material surfaces. This study was carried out using three types of Jotun epoxy coatings which are commonly used for coating water tanks in southern Iraq (one type used as undercoat primers). These epoxy-based coatings are: Penguard Primer COMP, A PM3192, epoxy primer based on a high molecular weight epoxy resin. This type is produced by Jotun Henry Clark Ltd, UK, and used as primer undercoats. Penguard HB consists of polyamide cured pure epoxy coating. This type of coats is referred as model A.Tankguard 412 consists from polyamine cured pure epoxy coating. This type of coats is referred as model B. The model's A and B of coatings are produced by Jotun paints Company of Emirates LLC, Sharjah, U.A.E.

## 1.2 Specimen preparation and coats

The material used for testing is the commercial stainless steel AISI 316 (EN 1.4401), widely used in the Iraqi cities to constrict water storage tanks. **Table 1** demonstrates the chemical composition of AISI 316 stainless steel (mass percentage) (Mika, 2013). The AISI 316 stainless steel has faced a cantered cubic crystalline structure. In addition to elements nickel, manganese, and nitrogen, this type of crystal structure makes it stabilizing and has more resistance to corrosion attack (Mackey, 2015). Under ISO Code 1143 standards (Gabriela, 2019) identical fatigue test samples are machined from AISI 316 plates. **Figures 1A** and **B** show the specific dimensions, sizes and geometry of the fatigue test specimens, respectively. **Figures 1C** and **D** indicate the specimen after the application of the two kinds of coatings. Initially, the test specimen's surface area is cleaned, dry, and the Penguard primer epoxy coating is applied. The two classes of Jotun coatings (models A and B) were applied by airless spray at nominally standard dry film thicknesses provided by the producer company. The primary function was to improve the adhesion of the epoxy-based coatings applied to the stainless steel surface. The coating thickness is evaluated by a paint thickness tester (Gain Express Holdings Ltd, China) to check coating thickness in the range of uses according to standard ASTM D1005-95 (David, 1999). At 25°C and atmospheric pressure, the coated specimens were left to cure for 14 days. A total of 15 specimens were used for testing in air, water, and gas environments.

**Table 1** The constituent elements of AISI 316 stainless Steel.

| Elements | Mass % |
|---|---|
| Cr | 0.08 |
| C | 0.08 mix. |
| Ni | 10-14 |
| N | 0.1 |
| Mn | 2 |
| Mo | 2-3 |
| Si | 0.75 |
| P | 0.045 |

*Sourece: Mika, 2013*

## 1.3 The fatigue test apparatus

The assembled apparatus used in the water environment fatigue test is gathered in a laboratory and shown in **Figure 2**. It comprises of a rotating-beam fatigue test machine SM 1090, Hi-Tech Ltd., UK. The fatigue test was conducted in a closed box with sizes of (35cm × 35cm × 25cm) by spraying the drinking water with a volume flow rate of 1 $m^3$/h at the atmosphere's pressure and temperature. All fatigue tests were performed under the rotating bending stress ratio ($\sigma_{min}/\sigma_{max}$ =0.5) and fatigue cycles within the range of $10^1$ to$10^7$ cycles. **Figure 3** shows the collected fatigue testing device used in gaseous environments. Besides the gas bottle used as $CO_2$, $H_2S$, and $SO_2$ gas sources, the same rotating-beam fatigue testing machine and the same closed box size are used. The percentage increase or reduction rate of fatigue limits (% $FL$) for applied epoxy base coatings under various gaseous and water environments were calculated by the formula (Bhuiyana *et al.*, 2010):

$$\% FL = \frac{\sigma_c - \sigma_{uc}}{\sigma_{uc}} \quad (1)$$

Where $\sigma_c$ and $\sigma_{uc}$ are the fatigue limits of the coated and uncoated specimens respectively which obtained from the S-N curves.

### 1.4 Porosity of epoxy based coatings

Different techniques are found to estimate the porosity of epoxy-based coatings (Fernanda *et al.*, 2000; Asep *et al.*, 2017). The simple technique is used in determining the porosity from bulk volume (*Vb*) and pore volume (*Vp*). The quantity of bulk volume (*Vb*) is determined using direct weighting ASTM E1920-03 (Mitchell, 2018). A cavity is produced by this technique in a cylindrical specimen and is filled with epoxy based coating. The sample is drawn and weighed after drying. The sample is then put in a glass beaker, and the fluid volume that the sample displaces is determined volumetrically. This volume is represented by the bulk volume (*Vb*). The volume of the pore in the epoxy coating is determined by the fluid saturation method. In this method, the dry specimen is weighted and placed in potable water until saturation occurs. The weight difference between the situated case and the dry case is taken and divide by water density to determine pore volume (Vp). The porosity (∅) can be acquired through the following relationship (Poovanna *et al.*, 2018):

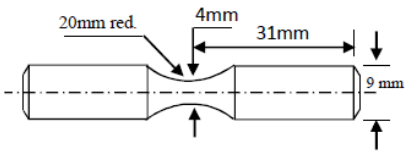


A-Shape and dimension of the specimen

B- Specimen before coating

C- Model A coating

D- Model B coating

**Fig. 1** Specimens for fatigue test under different environments

$$\emptyset = \frac{V_p}{V_b} \quad (2)$$

## 2 Results and Discussion

The fatigue tests for stainless steels in cases of uncoated and coated by the epoxy-based coatings in different environments were conducted at a stress ratio of 0.5 and a testing frequency of 50 Hz by rotating bending fatigue testing machine, and the results acquired illustrate in **Figures 4, 5 and 6** respectively. As shown in Fig. 4, 5, and 6, all cases' S-N curves have a similar shape and inclination. It is also seen that at the beginning of fatigue test in water media, i.e., at high-stress level, a large drop in fatigue life up to $10^2$ cycles, but after this cycle, a large drop of oscillates occurs continuously until specimen failure.

The S-N curves have shown that the tested stainless steel's fatigue properties were enhanced after applied the epoxy-based coatings compared with that of the uncoated stainless steel. These improvements in fatigue properties' characteristics have been attributed to the epoxy-based coating that covered the steel substrate and will reduce the processes of deformation and cracks initiation throughout the fatigue test. This, the epoxy-based coating do on increased and supported the strength of the stainless steel.

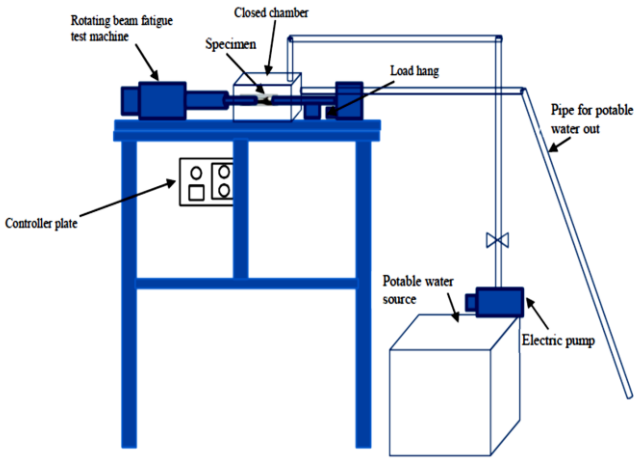


**Fig. 2** Schematic setup of fatigue testing apparatus under water environment.

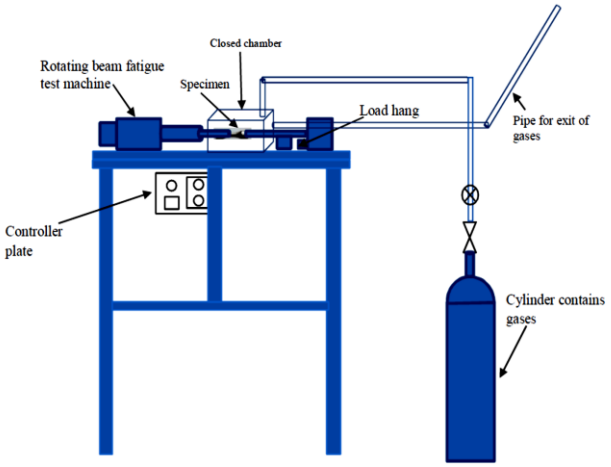


**Fig. 3** Schematic setup of fatigue test under air and gaseous environments.

From **Figures 4, 5,** and **6** can be seen the influence of the test environment on the fatigue behavior and reduces the fatigue life and strength of both types of epoxy-based coatings. The effects of $CO_2$, $H_2S$, and $SO_2$ gases are small compared to the influence of potable water. Also, $CO_2$ gas has the most significant impact, whereas $SO_2$ gas has the lowest impact and $H_2S$ gas has an intermediate effect on fatigue life and strength of steel and its coatings. This is attributed to various factors, including diffusion, adsorption, and molecular structure of both gases and coatings. The coatings will minimize hydrogen gas interaction from water or hydrogen sulfide and stainless steel substrate and reduce hydrogen gas's absorption process. This minimizes the Hydrogen embrittlement process of stainless steel (Thorsten *et al.*, 2009).

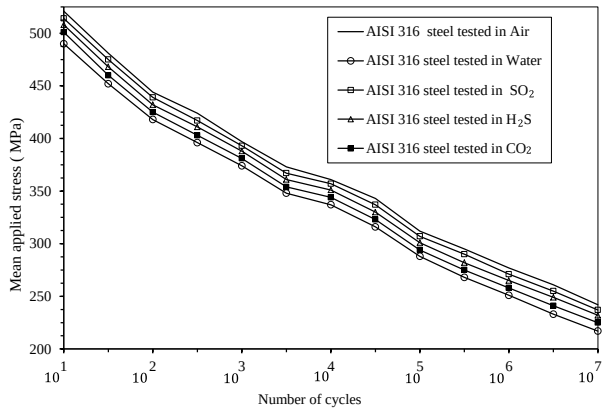


**Fig. 4** S-N curves of stainless steel AISI 316 tested in different environments.

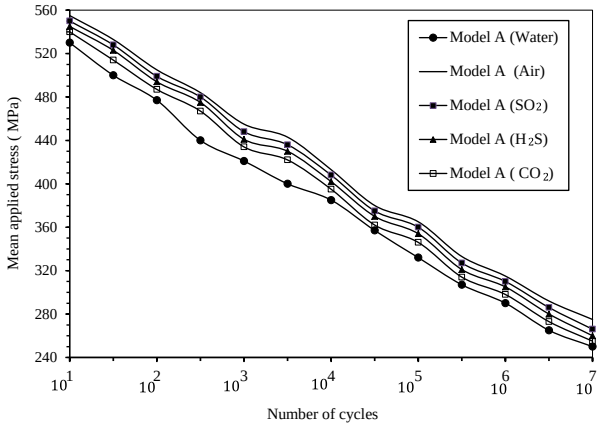


**Fig. 5** S-N curves of AISI 316 steel coated by model A tested in different environments

As shown in Fig. 4, 5, and 6, the implemented epoxy-based coating will increase the fatigue limit and improve fatigue resistance compared to the uncoated AISI 316 stainless steel. The epoxy coatings applied are a barrier to multiple impurities in drinking water that contribute to stainless steel pits' initiation and become notches for the crack initiation and propagation and influence steel's fatigue characteristics. A potable water environment decreases the fatigue limit and life of both coated and uncoated stainless steel. This is because the water molecules pass through the layer's thickness and reduce the bond strength between the epoxy-based coating compounds themselves and the deposition force between the layer and the steel substratum. Usually, this reduction in the bond strength will enhance a crack generation through the thickness of the coating and spread to the steel

Substratum and increase fatigue failures. The diffusion and adsorption of molecular gases by coating surfaces are the most significant factors affecting the fatigue life and fatigue strength of the coatings in $SO_2$, $CO_2$, and $H_2S$ environments. The adsorption of gasses by coatings results in a rise in the slip of coatings molecules, which supported cracks propagation during the fatigue test. In addition, the hydrogen molecules can be offered by the $H_2S$ gas that leads to coatings material degradation under cyclic load, sometimes relates to the hydrogen molecules as embrittlement that decreases the fatigue resistance and life of coated and uncoated stainless steel. In addition to the durability and strength that the coatings add to the test samples, it reduces the contact between gases or fluids with the samples during the test, and this raises the value of the impacted load and stress during the test and thus raises the value of the resulting fatigue life, and also increases the period needed by the crack to grow and spread. The improvement in fatigue resistance and fatigue life was found depending on the type of coating used, its components, and thickness of the coating, adhesive strength, and test conditions. It was found through the test that the brittleness of the polyamide coating is greater than that of the polyamine, and this makes the crack growth faster in polyamide coating compared to the polyamine coating, and this mainly depends on the thickness and porosity of the coating, which will be explained in detail in the next paragraph.

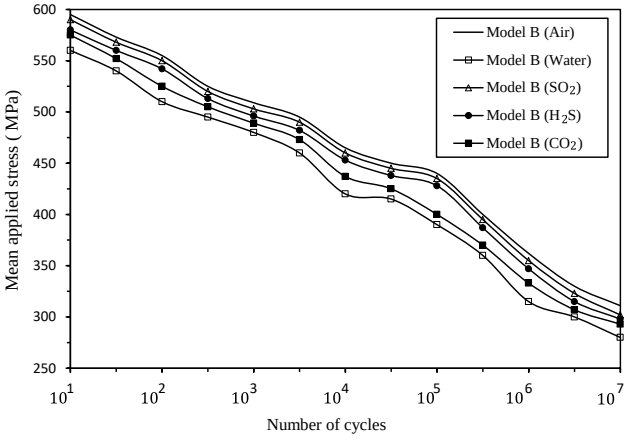


**Fig. 6** S-N curves of coated AISI 316 steel by model B tested in different environments.

As shown in Fig. 4, 5, and 6, all the coated and uncoated test specimens are not fractured at $10^7$ cycles but more than $10^7$ cycles. This, cycle $10^7$ is considered for estimating the fatigue limits values. Table 2 outlined the values of fatigue lime obtained from Fig. 4, 5, and 6. As appeared in Table 2, the fatigue limit values obtained from fatigue tests conducted in the water environment are smaller than those obtained from fatigue tests conducted in the air and gases environments. Model A coating contains polyamide epoxy-based coats is less fatigue-limit compared to model B containing polyamine epoxy coats. The drinking water will reduce the fatigue limit values acquired from performed fatigue tests of both uncoated and coated AISI 316 stainless steel. The percentage increase in the fatigue limits are computed by Eq.(1) for both models of epoxy-based coatings, and the results are summarized in **Table 3**. As shown in Table 3, there is a distinction in percentage increase in the fatigue limits owing to the impact of air and water media in coatings. The water presentation increases the coating degradation, which enhances pits initiations that become defects to develop cracks in specimens, which reduces fatigue limits.

**Table 2** Fatigue limits obtained from fatigue test at gases and water environments

| Environments | Fatigue limit values (MPa) | | |
|---|---|---|---|
| | Uncoated | Model A | Model B |
| Air | 240 | 275 | 311 |
| Water | 221 | 250 | 280 |
| $SO_2$ gas | 236 | 266 | 303 |
| $H_2S$ gas | 230 | 260 | 298 |
| $CO_2$ gas | 227 | 255 | 292 |

**Table 3** The percentage increase in fatigue limits in different environments.

| Environments | Increases rate of fatigue limit % | |
|---|---|---|
| | Model A | Model B |
| Air | 14.58 | 29.58 |
| Potable water | 13.12 | 26.69 |
| $SO_2$ gas | 12.711 | 28.39 |
| $H_2S$ gas | 13.04 | 29.56 |
| $CO_2$ | 12.33 | 28.63 |

Dry air environment involves different gasses like $H_2$, $O_2$, $N_2$ ...etc. These gasses have an essential impact on fatigue characteristics through the diffusion process, depending on their concentration. Then it affects the nucleation and initiation of cracks. The $N_2$ gas has chemical interaction with stainless steel alloy elements and creates different phases inside stainless steel material, affecting fatigue strength (Lin *et al.*, 2005). The diffusion rate of hydrogen in the stainless steel material enabled the hydrogen to migrate at the crack tip and enhanced the hydrogen embrittlement's consequence that increases the crack growth rate (Chopra *et al.*, 2001). The oxygen assists the crack propagation in stainless steel related to the composition and microstructure of stainless steel. The oxygen increases the localized deformation at the crack faces and tips while carrying out the air environment test (Jiang *et al.*, 2017). The reaction between polyamine and polyamide epoxy coatings with $SO_2$ gases can be represented by the following chemical reactions (Lv *et al.*, 2012; Khoma *et al.*, 2005):

$$R - NH_2 + SO_2 + H_2O \longrightarrow R - NH_3^+ + H^+ + SO_3 \quad (3)$$
$$R - CO - (NH)_2 + SO_2 + 2H_2O \longrightarrow H_2O - CO(NH)_2 - SO_2 + R - OH + H^+ \quad (4)$$

As is clear from these two reactions, the $SO_2$ is reduced to hydrogen ions, which have deteriorating effects and causes a flaw in the epoxy coating, this the growth of the fatigue crack is enhanced. In general, sulfur dioxide was diffusion or penetrant through defects such as fissures, micro-cracks, and pores in polyamine or polyamide epoxy coatings. This resulted in coating film properties on the interfacial bonding of epoxy-coated steel and accelerated both the deformation and crack growth during the test (Moverare *et al.*). The reaction between polyamines and polyamide epoxy coating with $CO_2$ gases can be represented by the following chemical reactions (Sinda *et al.*, 2018; Vega *et al.*, 2016; Michele, 2016):

$$R - NH_2 + CO_2 \longrightarrow R - NH_2^+COO^- \quad (5)$$
$$R - CO - (NH)_2 + CO_2 + 2H_2O \longrightarrow H_2O - CO(NH)_2 - CO_2 + R - OH + H^+ \quad (6)$$

The $CO_2$ molecules penetrate the polyamine or polyamide epoxy coating and accumulate to construct big bubbles that can lead to construct surface or internal defects and destroy the coating properties and reduce the coating's resistance to crack propagation (Yao *et al.*, 2018).

The reaction between polyamines and polyamide epoxy coating with $H_2S$ gases can be represented by the following chemical reactions (Sinda *et al.*, 2018; Matthew *et al.*, 2016):

$$R - NH_2 + H_2S \longrightarrow R - NH_3^+ + HS^- \quad (7)$$
$$R - CO - NHR + H_2S \longrightarrow R - COHS + R - NH_2 \quad (8)$$

The contact with hydrogen sulfide ($H_2S$) with epoxy coating causes coating deterioration due to absorption and reaction, which is significantly influenced by fatigue behavior and assisted cracking and damage (Noor *et al.*, 2016). Hydrogen embrittlement is divided into three kinds: hydrogen reaction embrittlement, internally reversible hydrogen embrittlement, and hydrogen environment embrittlement. Due to the direct contact of water or gases with epoxy coating, the hydrogen reaction embrittlement type is dominant. The hydrogen enhanced decohesion (HEDE) mechanism involves absorbed of hydrogen gas at crack faces and tip. Suppose the concentration of hydrogen in the crack faces and tip is sufficiently high to reduce the strength of the interatomic interactions in the substrate. In that case, cleavage of the crack tip bonds occurs under reduced stress. The combination of high stress, sharp crack tip, and high hydrogen concentration at the crack faces and the tip is required for the hydrogen-enhanced decohesion mechanism to be applicable (Gangloff, 2008). The reaction between polyamines and polyamide epoxy coating with water can be represented by the following chemical reactions (Jose *et al.*, 2017; Sinda *et al.*, 2018):

$$R - NH_2 + H_2O \longrightarrow R - NH_3^+ + OH^- \quad (9)$$
$$\text{R-CO-NHR} + H_2O \longrightarrow \text{RCOOH} + \text{R-NH}_2 \quad (10)$$

Each sort of elemental composition of the epoxy-based coatings affects the fatigue limit. Polyamines are essentially made up of ammonia with one or more nitrogen atoms and alkyl groups of hydrogen. The hydrogen atoms are connected by hydrogen bonds, while a Van Der Waals bond links the nitrogen atoms and the alkyl group (Jan *et al.*, 2006). The absorption and diffusion of water through a layer thickness of Polyamine coating causes the volume of coating to increase. The water molecules diffusion could interrupt Van Der Waals bonds between coating components. The water absorption in coatings has destroyed the bond at the interface between the coating and steel material. This generates additional cavities at the interface between them. This affects the efficiency of fatigue resistance and reduces the fatigue limit values. The coating of polyamides is a crystalline material consisting essentially of hydrogen ammonia, a carbon/oxygen atom, and an alkyl group (Gula *et al.*, 2016). The immiscibility of the polyamides coating in drinking water can lead the water molecular to inter-diffusion through coatings, resulting in a fragile interface between the coating layer and the surface of stainless steel that reflects the low fatigue strength and fatigue limit of the polyamides coating. Also, water diffusion through the Polyamines coating is less compared to Polyamides epoxy-based coating (Petr, 2001; Saikat, 2008).

The basic fatigue characteristics of AISI 316 stainless steel depending on the chemical compositions. The majority of the AISI 316 stainless steel alloying elements are listed in Table 1 contributes to the improved fatigue properties. (Brnic *et al.*, 2016; Benselya *et al.*, 2009). Among these elements added to AISI 316 stainless steel, only the chromium has adverse effects on the fatigue strength, but it is improved the resistance of stainless steel to corrosion (Alexander *et a*l., 2010).

To test and compare the effect of porosity of the two types of epoxy based coatings in fatigue properties, both the bulk volume (*Vb*) and pore volume (*Vp*) are measured using the approaches explained in section 1.4. Then, The porosity as a percentage value is calculated utilized Eq.(2), and the results are outlined in **Table 4**. It is clear from the data summarized in Table 4 that model B has the lowest value of porosity while modeling A has a more excellent porosity value. It is also shown that there is a large difference in porosity values between the two types of epoxy-based coatings. As the percentage values of porosity decreases, the fatigue life and fatigue limit are enhanced since porosity in the coatings serves as points for the concentration of stress and becomes a location for initiating cracks vicinity the test stainless steel surface and ultimately result enhances of fatigue failure. The microscopic observation of the specimens tested after a fracture was carried out to study and describes the mechanism of crack propagation, fracture surface, and surface morphology impacts from environments. **Figures 7** and **8** illustrated the specimens after a fracture. As indicated in Fig. 7 and 8, there is a higher distinction in tested samples' fracture surfaces in gasses and water media. All characters are coverage by damage and pits speared on the specimen surfaces. The impact of water with crack faces will help accelerate the crack's growth during a fatigue test. Alternatively, the water has access to the different concave areas in the coatings. Due to cyclic loading effects, the micro-cracks' growth in the coating layer and specimens increases, which accelerates the failure. More damage and loss of epoxy-based coatings are presented in most tested specimens in water media than those tested in gas media. It is discovered that there is an increase in pits produced owing to the water effect during fatigue cycles in water media. When these pits reach a critical size; it is starting to grow and propagate as cracks.

**Table 4** The porosity of the two models of epoxy-based coatings.

| Property | Models of coatings | |
|---|---|---|
| | Model A | Model B |
| Porosity % | 11.17 | 8.32 |

Both models of coatings tested in $CO_2$ gas media have more pits than other gases. As shown in Fig. 8. The specimen surface covered by model B coats tested in $CO_2$ gas has more pits spreads on the surface than those tested in $SO_2$ and $H_2S$ gases. The surface characteristics of fractured coated specimens illustrated a distinct mechanism for creating fatigue crack during fatigue testing, and the types of media used for the testing influence it. First, in the shape of a peripheral, a circular crack can produce and spread within the specimens, and a sharp edge characterizes this type. The second kinds of fatigue crack are generated due to the coating, and stainless steel itself defects such as bubbles and pores in stainless steel and coating. This type is started inside the coating materials and spread toward various directions during fatigue tested. The third form of a fatigue crack is developed in the middle of the specimen as a slit and then distributed across the specimen in a diagonally inclined path owing to cyclic loading impacts until the specimen fractures occur.

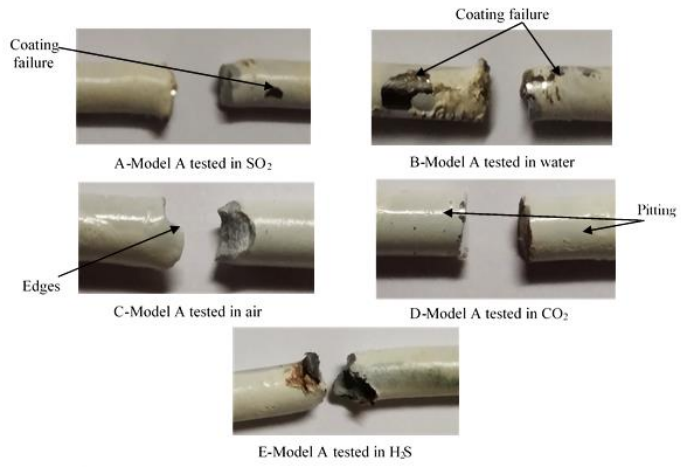


**Fig. 7** The fractured surface of model A specimens after test in different environments

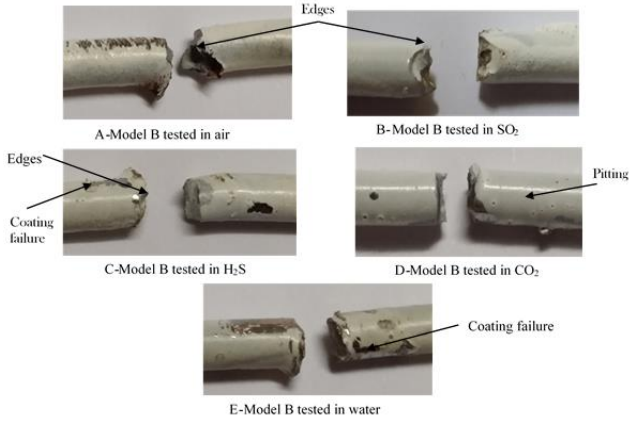


**Fig. 8** The fractured surface of model B specimens after test in different environments

## Conclusions

Fatigue experiments were carried out in the water, air, $CO_2$, $H_2S$, and $SO_2$ gases to understand the fundamental fatigue characteristics of AISI 316 stainless steel and epoxy-based coatings. From the results, it has been found that the applied epoxy based coatings increase the fatigue limits and fatigue life of stainless steel. The fatigue limit of epoxy-based coatings tests in the air environment is more significant than that acquired from tested in the presence of gaseous and water environments. Also, for $CO_2$, $H_2S$, and $SO_2$ gases, the $CO_2$ gas has the most significant impact, whereas $SO_2$ gas has the smallest effect and $H_2S$ gas has an intermediate influence on fatigue life and strength of steel and its coatings. The Environments affect the mechanism for initiating and propagating fatigue cracks, and it is distinct from one environment to another. The fatigue limit of the coatings based on polyamine epoxy is higher than the coating based on polyamide epoxy. This is attributed to various individual factors related to composition, properties, and tendency to react with the environment types of epoxy-based coatings.

### Nomenclature

| | | |
|---|---|---|
| $\% FL$ | =The percentage increase or reduction rate of fatigue limits | [%] |
| $\sigma_c$ | =The fatigue limits of the coated specimens | [MPa] |
| $\sigma_{uc}$ | =The fatigue limits of the uncoated specimens | [MPa] |
| $V_b$ | =Bulk volume of epoxy coating | [$cm^3$] |
| $V_p$ | =Pore volume of epoxy coating | [$cm^3$] |
| ($\emptyset$) | =The porosity OF epoxy coating | [%] |
| R | =Function groups | [-] |

## References


Alexander, M., Alban J., Aníbal S., and U. Ivan "Development of a correlation to estimate the fatigue strength for steels based on low-cost tests," *J. of CT and F-Ciencia Tecnología Y Futuro*, **2**, 1-12 (2010).

Asep, B., and Kikuo O. "Influences of size and amount of colloidal template and droplet diameter on the formation of porous-structured hyaluronic acid particles", *Indonesian J. of Sci. and Tech.*, **2**, 152-165 (2017).

Avery, R., Lamb S., Powl C., and Tuthill A. "Stainless steel for potable water treatment plant," *NIDI technical serious*, **10089**, 1-8 (1999).

Bensely, A., Shyamala L., Harish S., Mohan D., Nagarajan G., Krzysztof J., and Rajadurai A. "Fatigue behaviour and fracture mechanism of cryogenically treated En 353 steel", *Materials and Design*, **30**, 2955-296 (2009).

Bhuiyana, M., S., Ostukab Y., Mutohb Y., Muraic T., and Iwakam S. "Corrosion fatigue behavior of conversion coated AZ61 magnesium allo", *Mat. Sci. and Eng.*, **18**, 4978-4984 (2010).

Bruck, S., Volker S., Martina S., Hans J. C., Claus P., and Stefan W. "Hydrogen embrittlement mechanism in fatigue behavior of austenitic and martensitic stainless steels", *Metal*, **8**, 1-19 (2018).

Brnic, J., Turkalj G., Canadija M., Lanc D., Krscanski S., Brcic M., Li Q., and Niu J. "Mechanical properties, short time creep and fatigue of an austenitic steel", *Materials*, **298**, 1-19(2016).

Chopra, O., and Shack W. "Environmental effects on fatigue crack initiation in piping and pressure vessel steels," *NUREG/CR-6717*, **27**, 1-86 (2001).

David, B. "Coating thickness measurement", *Metal Finishing*, **97**, 545-550 (1999).

Edward, R., and Alaya F. "Bearing failure analysis on gearbox forced draft fan at LNG plant," *Indonesian J. of Sci. and Tech.*, **2,** 124-137 (2018).

Fernanda, A., Cristina L., Marcello R. and Paola M. "Techniques used to determine porosity", *American Ceramic Society Bulletin*, **7**, 49-52 (2000).

Foster, S., "Mechanochemical investigation of a glassy epoxy- amine thermoset subjected to fatigue", Ph.D. Thesis, University of Southern Mississippi, Mississippi, U.S, (2015).

Gabriela, M., R. Solis, Y. Gil, and Lozano D."Continuous estimation of the crack growth rate during rotating-bending fatigue testing", *Metals*, **9**, 2-9 (2019).

Gangloff, R. "Science-based prognosis to manage structural alloy performance in hydrogen, effects of hydrogen on materials", Proceedings of the 2008 International Hydrogen Conference, Jackson Lake Lodge, Wyoming, Harwell Oxford, UK, (2008).

Gula, S., Kausar A., Mehmood M., Muhammad B., and Jabeena S. "Progress on epoxy/polyamide and inorganic nanofiller-based hybrids: introduction, application, and future potential", *Polymer-Plastics Tech. and Eng.*, **17**, 1842–1862 (2016).

Ignatius, P, A. Bentang and Farid T. "Failure investigation of plastic shredding machine's flange coupling based on mechanical analysis", *Indonesian J. of Sci. and Tech.*, **2**, 124-133 (2017).

Jan, E., Nelson G. R., Lam K., and Thanh N. "Theoretical study on mechanism of epoxy amine cures reactions", *Macromolecules*, **40**, 4102-4105 (2007)

Jiang, R., Bull D.J., Proprentner D., Shollock B. and Reed P. "Effects of oxygen-related damage on dwell-fatigue crack propagation in a P/M Ni-based superalloy: From 2D to 3D assessment", *Int. J. of Fatigue*, **1**, 175-186 (2017).

Krauklis, A., Abedin I. and Andreas T. "Hygrothermal aging of amine epoxy: reversible static and fatigue properties", *Open Eng.*, **8**, 447–454(2018).

Khoma, R., Gavrilenko M., and Nikitin V. "Interaction of sulfur dioxide with aqueous solutions of amides," *Russian J. of General Chemistry*, **5**, 727-3733 (2005).

Kumar, A., Sowmya G., Kadali V., and Nethi R. "A review on fatigue failure in marine and naval applications", *Int. J. of Innov. Res. in Sci., Eng. and Tech.*, **9**, 9523-9528(2018).

Kumar, D., and Reddy A. "Study of mechanical behavior in austenitic stainless steel 316 in welded joints", *Int. J. Mech. Eng. and Rob. Res.*, **1**, 37-56 (2013).

Kurgan, N. "Effect of porosity and density on the mechanical and microstructural properties of sintered 316L stainless steel implant materials", *Mat. and Design*, **1**, 235-241(2014).

Lin, C., and Lon L. "Environmental effects on the fatigue behavior of an austenitic stainless steel", Proceeding International Conference on Fracture (ICF11), May (2005), Turin, Italy.

Lukas, P., Kunz L., and Bartos J. "Influence of the gaseous environment on fatigue crack propagation in an austenitic steel", *Mat. Sci. and Eng.*, **56**, 11-18 (1982).

Lv, Y., Yu X., Tu S., Yan J., and Dahlquist E. "Experimental studies on simultaneous removal of $CO_2$ and $SO_2$ in a polypropylene hollow fiber membrane contactor", *Appl. Energy*, 97, 283–288 (2012).

Mackey, E., T. Seacord, and Lamb S. "Guidelines for the use of stainless steel in the water and desalination industries", *Water Res. Foundation*, Colorado, (2015).

Matthew, D., and Michael D. "A Practical guide to working with $H_2S$ at the interface of chemistry and biology", *Chem. Soc. Rev*., **22**, 6108–6117 (2016).

Melia, G., Moghal J., Hicks C., Oubaha M., McCormack D., and Duffy B. "Investigation of the mechanical and thermal fatigue properties of hybrid sol–gel coatings applied to AA2024 substrates", *J. of Coatings Tech. Res.*, **6**, 1083-1094 (2016).

Michele, A., Angela D., and Eugenio Q., Reaction Mechanisms in Carbon Dioxide Conversion, 1st. Ed., Springer, New York, USA (2016).

Mika, S., Handbook of stainless steel, 7th Edn., Outovumpu OYJ Publisher, Finland, (2013).

Mitchell, R., Handbook of Environmental Degradation of Materials, 3rd ed., 469-488, Elsevier B.V., U.K. (2018).

Poovanna, C., Asish K. P., Upendra K. Pandey, Claire M., Pradip D., and Majid B. " A new approach to compute the porosity and surface roughness of porous coated capillary-assisted low pressure evaporators", *Scientific Rep*., **11708**, 1-11, (2018).

Moverare, J., G. Leijon, and Palmert F. "Effect of $SO_2$ and water vapour on the low-cycle fatigue properties of nickel-base super-alloys at elevated temperature", *Materials Science*, **564**, 107-115 (2013).

Nandiyanto, A., Triawan F., Firly R., Abdullah A., Aono Y., Inaba K., and Kishimoto K. "Identification of micro-mechanical characteristics of monoclinic tungsten trioxide microparticles by nanoindentation technique", *Materials Phys. and Mech.*, **3**, 323-329 (2019).

Noor, A., C. Ismail, and Zakaria M. "The effect of hydrogen diffusivities on pani-modified epoxy coating under potentiostatic charging", *ARPN J. of Eng. and Appl. Sci.*, **11**, 1-7 (2016).

Romero, J., Ventura F, and Gomez M. "Characterization of paint samples used in drinking water reservoirs: identification of endocrine disruptor compounds", *J. of Chromatographic Sci.*, **40**, 191-197(2012).

Petr, K. "Chemical-resistance values of epoxy resins hardened with polyamines", *Pigment and Resin Tech.*, **3**, 150-158 (2001).

Sadananda, K., and Holtz R. "Review of fatigue of coatings/substrates", in Nanostructured Films and Coatings, 1st Edn., 198-201, Kluwer Academic Publishers, Springer, USA (2000).

Saikat, S. "Water absorption and dielectric properties of Epoxy insulation", M.Sc. Thesis, Norwegian University of Science and Technology, USA, (2008).

Shan, Z., Shujuan W., Chenchen S., and Changhe C. "$SO_2$ effect on degradation of MEA and some other amines", *Energy Procedia*, **37**, 896 – 904 (2013).

Sinda, L., Dubois L., Weireld G. De., and Thomas D. "Simultaneous absorption of $SO_2$ and $CO_2$ from conventional and partial oxy-fuel cement plant flue gases", *Chem. Eng. Trans.*, **69**, 1-6 (2018).

Thorsten, M., and Naumann J. "Coatings to reduce hydrogen environment embrittlement of 304 austenitic stainless steel", *Surface and Coatings Technology*, **203**, 1819-1828 (2009).

Vega, F., Sanna A., Maroto M., Navarrete B., and Abad D. "Study of the MEA degradation in a $CO_2$ capture process based on partial oxy-combustion approach", *IJGGC*, **54**, 160–167(2016).

Yao, B., Qiu-S., Shu L., and Li X. "Formation of $CO_2$ bubbles in epoxy resin coatings: A DFT study", *J. of Molec. Graphics and Modeling*, **86**, 1-14 (2018).

Wray, L., Ayre D., Irving P., Jackson P., Jones P., and Zhao F. "Implications of substrate geometry and coating thickness on the cracking resistance of polymer-based protective coatings," *Procedia Struct. Integrity*, **13**, 1768-1773 (2018).